Surface-chemical and -morphological gradients

Sara Morgenthaler, Christian Zink and Nicholas D. Spencer*

Surface gradients of chemistry or morphology represent powerful tools for the high-throughput investigation of interfacial phenomena in the areas of physics, chemistry, materials science and biology. A wide variety of methods for the fabrication of such gradients has been developed in recent years, relying on principles ranging from diffusion to time-dependent irradiation in order to achieve a gradual change of a particular parameter across a surface. In this review we have endeavoured to cover the principal fabrication approaches for surface-chemical and surface-morphological gradients that have been described in the literature, and to provide examples of their applications in a variety of different fields.

1. Introduction

Surface gradients are surfaces with chemical or physical properties that gradually change over a given distance. A gradual change in a physical property, such as the wettability, can be induced by a change in surface chemistry, for example a gradually changing surface composition.

The motivation to prepare gradients is two-fold. Gradients are, on the one hand, ubiquitous in nature and thus biomimetic gradients allow us to gain a deeper insight into biological processes. Concentration gradients across membranes are central to energy generation in cells, and biomolecule gradients direct the haptotaxis of cells, for example, in axonal outgrowth. In order to understand these processes more clearly one needs to mimic the *in vivo* situation in the lab, which requires controlled chemical gradients. In addition, gradients can be a valuable materials research tool that allows high-throughput and cost-effective analysis of the influence of a wide range of parameters in the minimum amount of time.

The influence of surface properties, such as wettability, on the attachment and growth of cells and bacteria, the adhesion of

Laboratory for Surface Science and Technology, Department of Materials, ETH Zurich, Wolfgang-Pauli-Strasse 10, CH-8093 Zurich, Switzerland. E-mail: spencer@mat.ethz.ch; Tel: +41-44-632-5850

proteins, as well as adhesion phenomena in general have traditionally been studied using series of individual samples. A large number of samples is typically prepared, each having a different surface property. This approach, however, has several disadvantages; different samples are prone to show a distribution of other properties, such as substrate roughness. It can therefore be difficult to attribute a particular effect to one single varying parameter, thus introducing a potential source of error, necessitating many repeat experiments. Furthermore, the handling of many samples means that experiments are time consuming. This is particularly problematic when working with biological specimens, since they may change their properties with time. Finally, multiple repeated studies extending over a long period of time may also encounter a range of different ambient conditions, which may influence the outcome of the experiments. By incorporating a range of surface properties into one single surface gradient, the need for lengthy repetitive procedures is avoided and many of these problems can be overcome.

In general, surface-chemical gradients can be created in two ways. Either the outermost surface layer of a substrate is gradually modified, for example by irradiation with an energetic beam,[1,2] or by chemical etching[3] or a surface coating, such as a self-assembled monolayer or a thin polymer film, is attached to the surface in a gradual manner. Whereas the former approach was more popular in early studies (see reviews by Elwing and Golander[4]
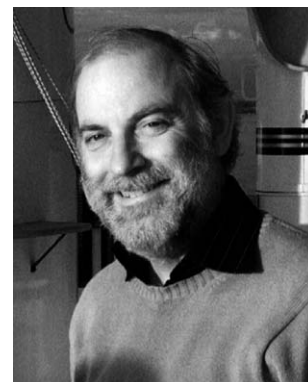
and Ruardy et al.[5]), the gradual application of surface coatings has become increasingly popular, since the bulk properties of the materials are less likely to be changed during this process.

Gradients have been applied in a large variety of studies, most often in those relevant to biomedical and biosensor applications, for example to investigate protein adsorption and cell adhesion[4,6–9] However, they have also been used in both fundamental and applied materials science studies, such as the growth of silane monolayers[10] or the generation of polymer libraries for sensor applications.[11]

We will first discuss the preparation methods that have been proposed in the literature and then cover the applications that have been addressed with surface gradients. The following section will be divided into the preparation of chemical gradients and the preparation of morphological gradients.

2. Preparation methods

2.1. Surface-chemical gradients

Surface-chemical gradients are mainly prepared via two systems: self-assembled monolayers (SAMs) or polymer coatings, especially brush-like polymer coatings—Table 1 provides an overview of the different preparation methods for the generation of surface-chemical gradients and the applications for which they have been used.

2.1.1. SAM-based techniques. SAM-based gradient preparation techniques can be divided into those developed for silanes on glass or silica surfaces and those applicable to alkanethiols on gold or silver.

Table 1 Surface-chemical gradient preparation techniques, systems and their applications

Technique		Adsorbate	Substrate	Application	References
Diffusion	Vapour phase	Silanes	Si, PDMS	Cell adhesion, protein adsorption, polymerisation template	10,13–21,55,56,62,63
	Solvent	Silanes	Si	Protein adsorption, polymerisation template	6,7,23–25,57,106,107,109,110
	Through a matrix	Alkanethiols, polymer	Au	Protein adsorption, cell adhesion	7,34–38,67
Printing	Contact	Alkanethiols	Au		47,48
		Silanes	Si		26
		Biomolecules	Funct. Si		82
	Ink jet	Alkanethiols	Au	Polymerisation template	49,50
		Proteins	Si		49
Desorption	By potential	Alkanethiols, polymers	Au	Cell adhesion, protein adsorption	39,40–43,74,80
	Concentration gradient	Proteins	Glass, Si, Au	Cell adhesion, further functionalisation	8,86–88
		Monomers	Funct. Si		75
		Monomer solution	Funct. Si	Solvent effect in copolymer brushes	65,66,68
Advancing solution		Proteins, biomolecules	Funct. Si, filter	Cell growth	83–85
	Controlling reaction time	Silane	Si	Polymerisation template, protein adsorption, cell adhesion	33
		Alkanethiols	Au		51–53
		Copolymer	Oxide surfaces	Protein adsorption	70
		—	PVC	Cell adhesion	3
	Depletion	Proteins	PDMS, glass		89,90
Irradiation	Change intensity	—	PE	Cell adhesion and growth, protein adsorption, polymerisation template	1,9,54,58–61,64
		Polyatomic ions	PMMA		12
		—	Polymer		2
	Change exposure time	Monomer solution	Funct. Si		69,77
		Proteins	Funct. PS		78,79
		Silane	Si, nanoporous Si	Protein adsorption, cell adhesion	29–32
	Through mask	Silane	Glass	Enzyme adsorption	27,28
		Monomer	Funct. Si	Cell adhesion	77
Temperature		Polymer	Funct. Si	Solvent, pH effects in copolymer brushes, protein adsorption, microtubule motion	71–73
Irradiation and replacement	Through mask	Alkanethiols	Au		44,45
	Change exposure time	Alkanethiols	Au		46
Physically controlled polymerisation	Plasma polymerisation (mask)	Polymer	Any		76
	Electropolymerisation (pot. gradient)	Polymer	Au	Cell adhesion	80

The most commonly used technique for silanes was developed in 1992 by Chaudhury and Whitesides,[13] who dissolved decyltrichlorosilane in paraffin oil and let it evaporate next to a silicon surface. The silane diffuses along the surface, partially adsorbs and generates a gradual change in coverage. This method has been used extensively by the groups of Chaudhury and Genzer. Chaudhury's group and others have used this approach to study the parameters that govern droplet movement along a wettability gradient.[14–17] Genzer et al. have used the silane-diffusion method to generate a wide range of gradients in chemical functionality, including gradients of polymerisation initiators that were subsequently used to generate brush-copolymer gradients.[10,18] The details for these techniques are provided in the following subsection on polymer-based techniques. Genzer and coworkers also varied the substrate, using both PDMS[19,20] and porous silica.[21] Silane gradients have also been prepared by diffusion through solvents. Elwing et al. were among the first to develop a gradient-preparation technique that used silane diffusion in liquids.[22] A solution of a short silane ($Cl_2(CH_3)_2Si$) dissolved in tricholoroethylene is covered by xylene. The two solvents slowly diffuse into each other, allowing the creation of a wettability gradient on an immersed silicon or glass substrate. Wettability gradients created by this method were used to study protein and polymer adsorption.[6,7,23–25] Other methods to generate wettability gradients from silanes include the use of microcontact printing to generate a gradual silane coating[26] and the gradual oxidation of silanes by UV irradiation through a density filter[27,28] or by varying irradiation time.[29–31] Han et al. created a gradient from superhydrophobic to superhydrophilic wetting by combining the gradual oxidation of a silane SAM with a nanoporous substrate, prepared by layer-by-layer assembly of negatively charged silica nanoparticles and positively charged poly(allylamine hydrochloride).[32] Gradients of silane-bound initiators that were further used for polymerisation were also created by pumping silane solution slowly into a vessel. By controlling the adsorption time for the silanes, a coverage gradient is generated.[33]

The first technique for generating alkanethiol gradients was developed in 1995 by Liedberg and Tengvall,[34] who again used a diffusion method to generate a gradient from two differently functionalised alkanethiols. They covered a gold substrate with a polysaccharide matrix and added different alkanethiol solutions behind glass frits, fixed at the two ends of the substrate, as shown in Fig. 1a. The alkanethiols were then left to diffuse for several hours, allowing them to generate a densely packed monolayer with a gradually changing end-functionality. These gradients were thoroughly characterised by ellipsometry, IR spectroscopy and X-ray photoelectron spectroscopy,[34,35] Fig. 1b. Order–disorder gradients[36] using alkanethiols of different lengths, and wettability gradients have been used to study protein adsorption and cell adhesion.[7,37,38]

In 2000, Terrill et al. presented a method that relied on the electrochemical desorption of alkanethiols from a fully covered SAM by application of a potential.[39] The width of the potential window and the position of the electrodes thereby determine the width and slope of the gradients (see Fig. 2). Alkanethiol gradients prepared by this method were used in a variety of other experiments, for example to test new mass-spectroscopic techniques,[40] to study cell adhesion,[41] or to investigate nanoparticle attachment.[42] In addition to electrochemical desorption,
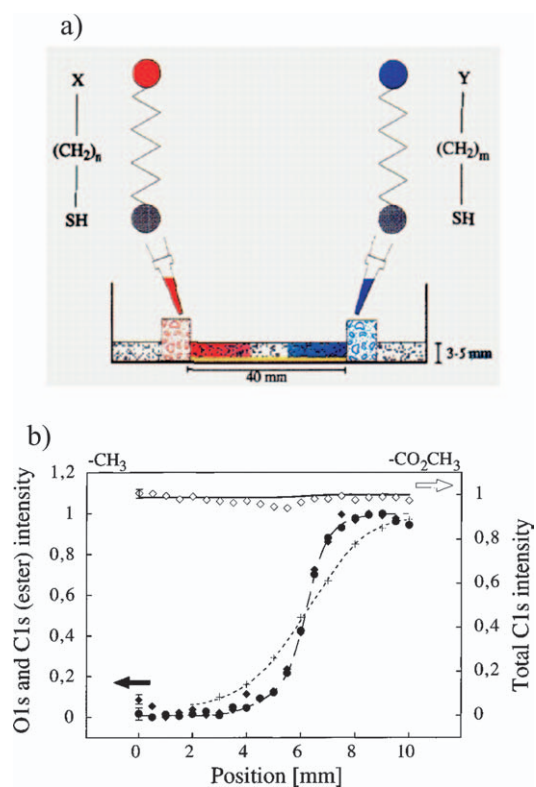

Fig. 1 (a) Schematic diagram of the cross-diffusion geometry used for the preparation of alkanethiol gradients on gold. Two alkanethiol solutions, placed behind glass filters, are left to cross-diffuse in a polysaccharide matrix.[34] (b) XPS intensity profiles obtained from a $HS(CH_2)_{15}CO_2CH_3$–$HS(CH_2)_{15}CH_3$ gradient prepared by this method. (●) O1s intensity, (◆) C1s (ester), obtained from the sum of the peak intensities of the four chemically shifted C1s peaks; (◇) total C1s intensity (282–292 eV). The profile clearly exhibits the characteristic shape of a diffusion process.[35]

alkanethiols have also been desorbed with a scanning tunneling microscope tip with a gradually increasing bias or scan speed.[43] One type of alkanethiol was desorbed from a full monolayer during the scanning process and replaced immediately by differently functionalised molecules from solution, which resulted in a two-component gradient in the submicrometre range.[43]

Photocatalytic oxidation, low-energy electrons or a focused X-ray beam have also been used to degrade alkanethiol SAMs in order to create surface-chemical gradients. Two-component gradients have been generated by Blondiaux et al.[44] Molecules from a full monolayer were gradually removed by oxygen radical oxidation and subsequently saturated with a second component. The oxygen radical concentration gradient was generated by UV irradiation of a thin TiO_2 film through a gray-tone photomask. In this way, repeating gradients in the micrometre range were created, which could be visualised via the contact line of a water droplet (see Fig. 3). A related technique presented by Ballav et al. used a variable dose of low-energy electrons to modify the SAM surface.[45] The exchange process during the subsequent immersion into a second component depended on the irradiation dose, thus leading to a higher exchange rate at the highly irradiated region. This allowed the creation of, for example, a wettability gradient. The desorption of alkanethiols by a focused X-ray
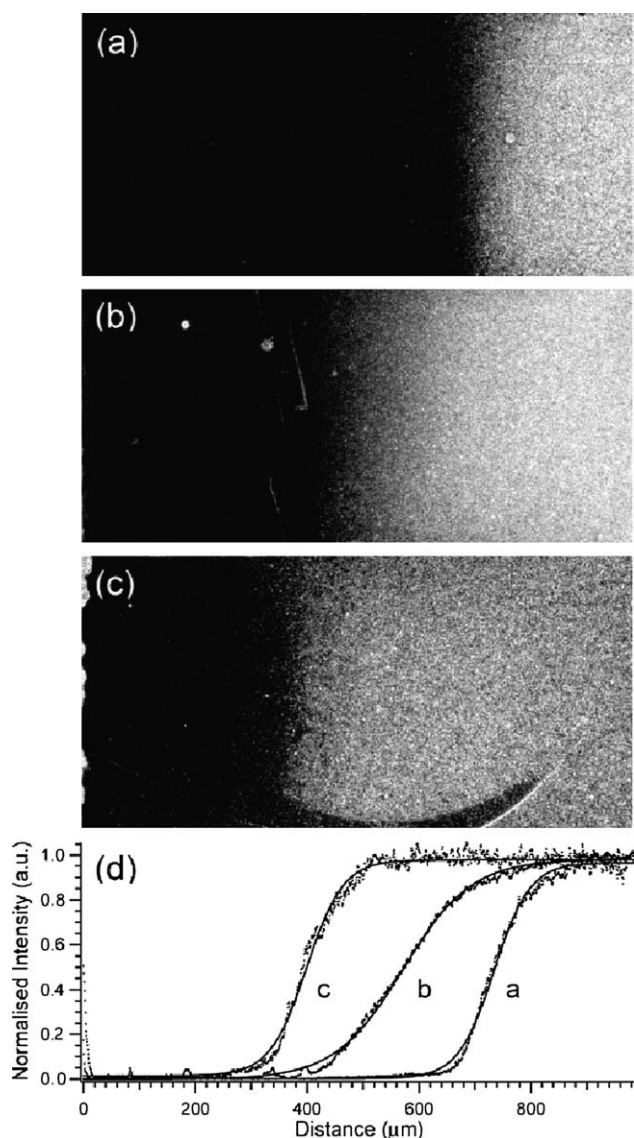
Fig. 2 Fluorescence images of nanosphere-tagged aminoethanethiol gradients prepared by electrochemical desorption with potential windows of (a) -1000 mV (left) $\leq V(x) \leq -200$ mV (right), (b) -900 mV (left) $\leq V(x) \leq -200$ mV (right), and (c) -800 mV (left) $\leq V(x) \leq -200$ mV (right). (d) Normalised intensity as a function of position for each image, with dotted lines corresponding to data and solid lines to fits of the data.[41]

Fig. 3 Dark-field image of a single water droplet deposited on the surface bearing repeating 720 μm wettability (thiol–gold) gradients produced by photocatalytic lithography. The corresponding grayscale variation in the photomask is shown below the image.[44]

Fig. 4 Linear surface-chemical gradient prepared by contact-printing of alkanethiols onto gold with a thiol-saturated, wedge-shaped stamp. Surface composition according to XPS at three lateral positions along a single gradient.[47]

beam has been controlled by varying the exposure time.[46] However, only single-component gradients of a variety of alkanethiols have been created by this technique, *i.e.* without using a subsequent backfilling step.

Next to diffusion- and desorption-based techniques, another class of methods has been developed based on printing. Regular contact printing has been used to generate gradients with a wide variety of different shapes[47] by applying very thin, contoured, alkanethiol-saturated PDMS stamps to a substrate (see schematic in Fig. 4). More molecules are available in the thicker regions of the PDMS stamp than in the thinner areas, thus allowing the formation of a higher-surface-concentration layer in the thicker regions, whereas fewer alkanethiol molecules are adsorbed in the thinner areas. The thickness of the PDMS is
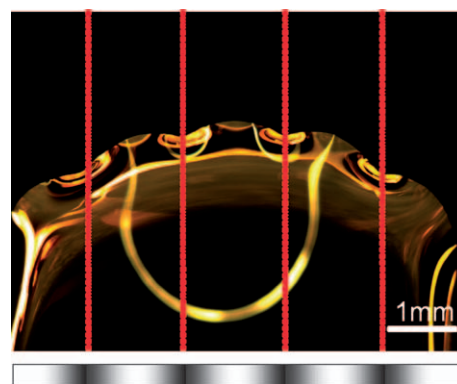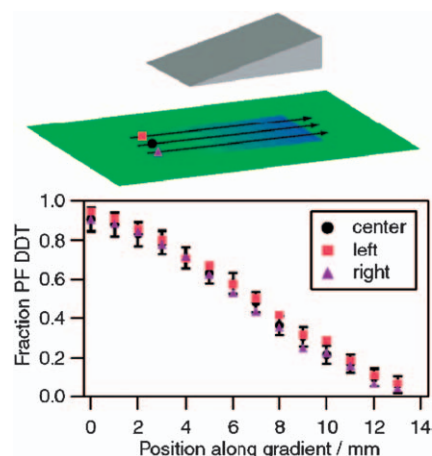
chosen to allow approximately one monolayer-equivalent of molecules to be present in the thickest regions. Geissler *et al.* also used contact printing to generate arrays of radial gradients in the nanometre range.[48] They printed a PDMS stamp saturated with a mixture of alkanethiols onto a particle array, allowing the diffusion of alkanethiols along the particles onto the surface. A radial gradient forms because of the different diffusion constants of the two alkanethiols. Ink-jet printing was also used to generate alkanethiol gradients in the centimetre range by printing one component and backfilling with a second.[49,50]

Finally, surface-chemical gradients can also be prepared by a two-step immersion process.[51] During the first immersion step a gradual change in surface concentration of one type of molecule, for example a methyl-terminated alkanethiol, is achieved by slowly immersing the substrate into a dilute solution of the adsorbate. The conditions are chosen such that longer immersion times (*i.e.* at the leading edge of the substrate) result in a densely packed monolayer assembly, whereas only very few molecules adsorb during short immersion times (*e.g.* at the trailing edge). By choosing an appropriate combination of concentration
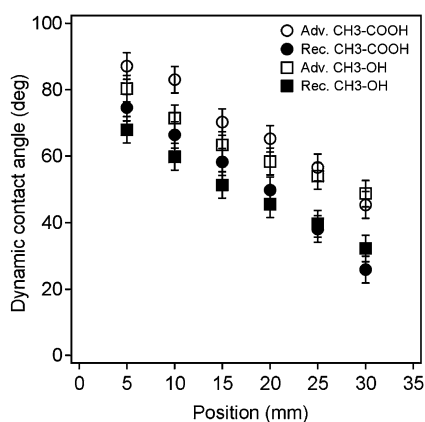
Fig. 5 Advancing (open symbols) and receding (filled symbols) water contact angles on a methyl-carboxyl (circles) and a methyl-hydroxyl (squares) gradient produced by the gradual immersion method (thiol–gold), measured along the major axis.[53]

and maximum immersion time, a coverage gradient of adsorbates can be created. This coverage gradient is mostly at submonolayer surface concentrations and can be saturated by subsequent total immersion of the substrate into a solution of a second type of adsorbate, for example a hydroxyl-terminated alkanethiol.[51] Such two-component gradients have an island-type submicrometre structure[52] but overall exhibit a high degree of molecular organisation.[53] Gradients with a linear change in wettability can readily be generated in this way, as shown in Fig. 5.

2.1.2. Polymer-based techniques. The polymer-based techniques can be again divided into two sections: those based on surface modification by, for example, irradiation and those based on the application of a gradually changing coating.

The review article by Ruardy et al. provides a good overview mainly of the creation of wettability gradients by surface modification.[5] Different types of surface irradiation, corona discharge or radio frequency plasma discharge, as well as etching solutions have been used to modify polymer surfaces. Gradients have been generated by either changing the time during which a surface is exposed to irradiation[2] or etching solution,[3] or by changing the irradiation power along the substrate.[1,54] During the exposure of the polymer substrate, a gradient in the concentration of activated oxygenated species is created on the surface, resulting in a gradient in wettability. However, all of these preparation methods have the drawback that the surface species generated are not well defined and that the substrates are also roughened during the process.

The number of techniques available to generate brush-like polymer gradients is large. The first part of this subsection will deal with the fabrication methods that employ silanes as grafting sites on the surface. The second part of the subsection covers all other techniques that allow brush-like polymer gradients to be created.

The silane-diffusion techniques developed by Chaudhury and Whitesides,[13] and Elwing et al.[22] have been used to generate gradients of grafting sites on silica surfaces. These grafting sites were used to either initiate the polymerisation of various monomers by atom transfer radical polymerisation (ATRP), a "grafting-from" technique,[55,56] or were used to attach PEG chains by the

"grafting-to" technique.[57] Brush-like polymer gradients were also generated from gradients of alkanethiol initiator sites applied by ink-jet printing.[50] Functionality gradients prepared by corona treatment were also further used to graft polymer chains. The oxygenated species were used as grafting sites for various polymers, such as PEG[58] or others.[59–61] Brush-like polymer gradients prepared by these techniques have been used to immobilise nanoparticles[62,63] and to study protein adsorption and cell adhesion.[59,64]

Other techniques begin with a homogeneous coverage in initiator density and control the polymerisation conditions, for example the polymerisation time. Tomlinson and Genzer used gradual draining of a monomer solution from a vessel to generate brush-like polymer gradients with a gradually changing molecular weight,[65,66] Fig. 6a, step A. A second polymer can be grafted from this MW gradient for the generation of a block-copolymer gradient, either by a similar draining step, which yields a block-copolymer brush with a constant thickness and gradually varying block length (Fig. 6a, steps D,E), or by complete immersion, which yields a gradient with gradually changing thickness but similar block length of the second component (Fig. 6a, steps B,C). Such block-copolymer gradients can also be prepared in an orthogonal way, leading to complete block-copolymer composition libraries, as shown in Fig. 6b. These have been used to study the effect of solvent on chain conformation. Other groups have used diffusion to control the adsorption time of a polymer during grafting. Mougin et al. allowed an NHS-functionalised PEG chain to diffuse through an agarose matrix—a similar approach to that developed by Liedberg for alkanethiols[34,67] whereas Xu et al. pumped a monomer solution slowly through a microchannel, controlling the contact time to generate a gradient in molecular weight.[68] Finally, a moving shutter has also been used to control the irradiation time of a mixed PEG methacrylate solution, which resulted in the generation of a crosslinked PEG thickness gradient that could be used for biosensor applications.[69] Polymer brush coverage gradients can also be prepared by controlling the adsorption kinetics of a brush-forming graft copolymer, for example poly(L-lysine)-g-poly(ethylene glycol) by a simple dipping technique[70] originally developed for the generation of alkanethiol gradients. After the generation of a coverage gradient, the surface can be easily saturated with a differently functionalised copolymer, which allows the creation of gradients from different functional groups, such as peptides or biotin. The effect of temperature on the grafting rate was exploited by Ionov et al.[71–73] They first coated a silica substrate with an anchoring layer of either silanes or a polymer and then a second layer of polymer. The degree of anchoring of the top-layer polymer, which was to form a brush-like coating, to the layer below is controlled by applying a temperature gradient. More chains are grafted to the surface at a higher temperature, thus allowing for the fabrication of a gradient in grafting density. Such gradients were used, for example, to study the behaviour of polyelectrolyte brushes at different pH values.[72] Full alkanethiol-initiator SAMs were also used for the preparation of mixed polymer brush gradients.[74] A first monomer, N-isopropylacrylamide, was polymerised on the full SAM by ATRP, then the polymer chains were desorbed by application of an electrochemical potential, as developed by Terrill et al.[39] Subsequently the empty sites were re-saturated with the initiator
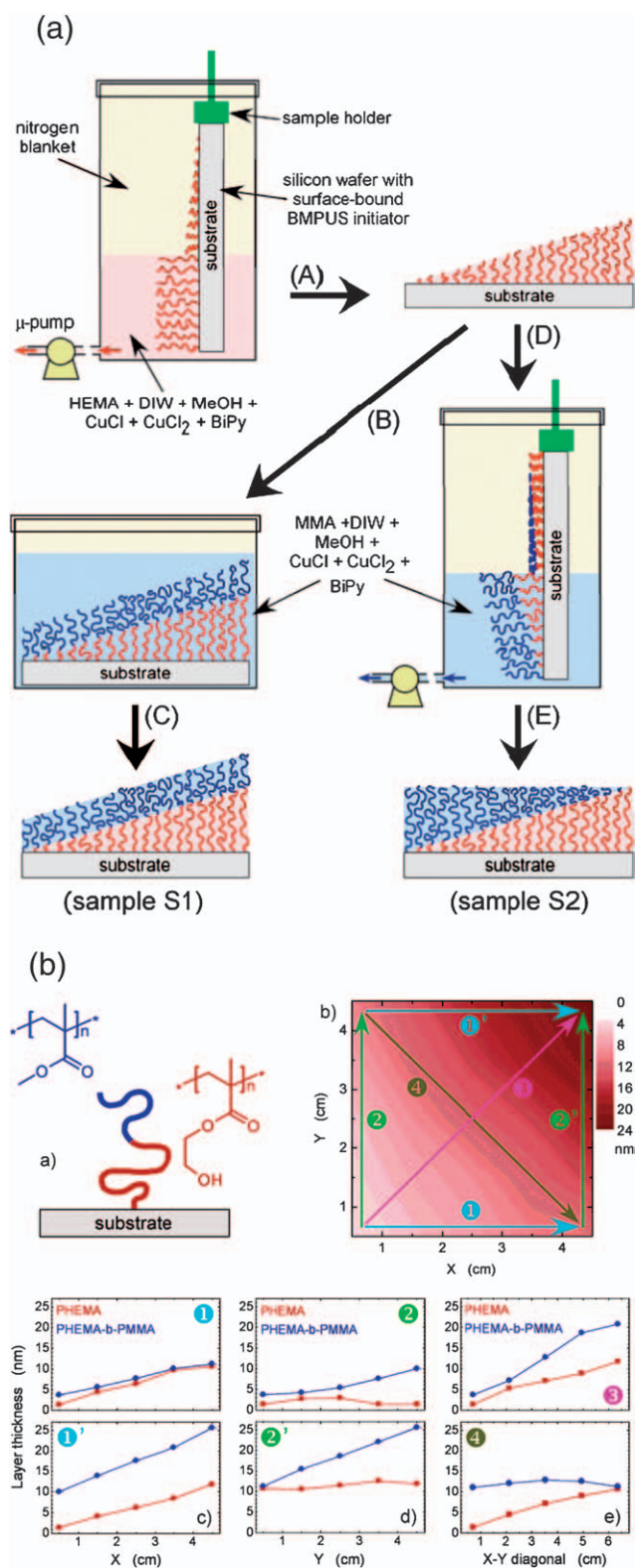
Fig. 6 (a) The preparation of surface-anchored PHEMA-*b*-PMMA gradients: a custom designed apparatus is used to decorate the sample surface with a grafted PHEMA having a gradient in molecular weight (arrow A). Surface-grafted PHEMA acts as a macroinitiator for the polymerisation of the PMMA block that has either a constant molecular weight (arrow B) or a variable molecular weight (arrow D). The overall process results in PHEMA-*b*-PMMA block copolymers with a constant

and a second monomer, for example 2-hydroxyethylmethacrylate, was polymerised, which led to the formation of a mixed polymer brush gradient.

Not only have polymerisation conditions been gradually varied, but also the composition of the monomers used for polymerisation has been gradually adjusted. Xu *et al.* created a concentration gradient of (*n*-butylmethacrylate and 2-(*N*, *N*-dimethylamino)ethylmethacrylate in a microchannel by gradually changing the infusion rates of the two solutions.[75] Atom transfer radical polymerisation (ATRP) then led to the generation of a brush-copolymer gradient. Whittle *et al.* used plasma polymerisation to generate a gradient in chemical functionality by gradually changing the composition of a plasma and at the same time gradually shielding the substrate.[76]

Various groups have used photoimmobilisation or photopolymerisation to generate brush-like polymer gradients by changing the dose of light, for example, with a photomask,[77] or by changing the irradiation time.[78,79]

Also an electropolymerisation process in the presence of an in-plane electrochemical potential gradient was further used to generate poly(acrylic acid) and poly(acrylamide) thickness gradients.[80] Subsequent surface derivatisation of such thickness gradients could be used to generate peptide, fluorinated or nanoparticle gradients.

Finally, not only polymers but also proteins have been immobilised on surfaces as a gradient. The attachment and movement of cells depends strongly on the surface concentration and the confirmation of adsorbed proteins, and thus it is useful to study this behaviour in a high-throughput manner. Proteins have been covalently coupled to alkanethiol gradients by, for example, an amine group[37,81] or by laser irradiation[78] and they have been ink-jet printed[50] or stamped.[82] Other groups have controlled the adsorption kinetics by changing the contact time of a substrate with a protein solution.[83,84] Controlled adsorption kinetics were also used to immobilise single-stranded DNA onto an indium–tin oxide surface,[85] which allows the generation of a biosensor surface. Finally, microfluidics have also been used to generate concentration gradients of molecules in microchannels. Whitesides' group has created gradients in proteins and other biomolecules by controlling the laminar-flow conditions and have investigated cell attachment and growth[8,86–88] on these surfaces, while the groups of Caelen and Fosser have used the depletion of protein solutions along microchannels to generate coverage gradients.[89,90]

2.2. Morphological gradients

Within the last decade, various approaches have been described to fabricate different kinds of morphological gradients, varying in feature shape and size, length and in the fundamental principle that is used to create them. In order to compare these techniques, those fabricated by similar basic principles have been grouped together.

PMMA length and a variable total length (arrow C) or a gradual PMMA length and a constant total length (arrow E).[65] (b) Dry thickness profile of PHEMA-*b*-PMMA MW1/MW2 orthogonal brush gradients as a function of the position on the substrate. (c–e) PHEMA (red squares) and total copolymer (blue circles) thicknesses along the directions depicted in the total thickness profile shown in part b.[66]

2.2.1. Particles. One widely used approach to create morphological gradients is to bind particles onto a smooth substrate. Genzer and his colleagues[62,66,91–93] have established a simple but highly efficient procedure to create nanofeature gradients by creating gradients of polymers and then adsorbing gold particles. They have employed two basic principles to create one-dimensional gradients or a combination of both to prepare two-dimensional gradients.

The first principle is the Chaudhury and Whitesides[13] procedure (see section 2.1.1), involving the evaporation of functionalised silanes next to a silicon substrate. If a silanised polymerisation initiator is used, this approach can produce a gradient in grafting density of polymer chains on the surface (see section 2.1.2). The second principle is simply withdrawing the polymerisation solution while the process is still running. The lower parts of the sample are thus grafted with longer chains, or in other words a gradient in molecular weight of the grafted polymer can be produced (see section 2.1.2). The particle gradient is produced by immersing a polymer gradient, such as poly(2-(dimethylamino) ethylmethacrylate) (PDMAEMA) into a gold nanoparticle suspension and letting the particles adsorb onto the polymer over several hours (see Fig. 7). Depending on the particle size, "quasi" 2D structures or 3D dispersions of nanoparticles can be achieved. Larger particles (diameter $\approx$ 16 nm) are not able to penentrate the polymer brush and they always remain in the top layer of the polymer. In order to form a 3D dispersion the particle size has to be reduced drastically (down to $\approx$ 3.5 nm) to allow the particles to penetrate throughout the thickness of the polymer brush.

Huwiler et al.[94] have developed a direct technique (i.e. not via a chemical gradient) for the fabrication of a nanoparticle density gradient by a simple dip-coating process. The principle was to adsorb negatively charged silica particles onto a positively charged surface (a poly(ethyleneimine) (PEI)-coated silicon wafer) by means of electrostatic interactions. Since the adsorption is a kinetically controlled process, a particle gradient can be created by exposing different parts of the substrate for increasing times to a colloidal suspension. This was achieved by slowly immersing the substrate into a colloidal suspension of silica nanoparticles, leading to a gradual increase in particle density along the substrate surface. In order to increase the mechanical stability of the particle array and to adjust their shape the gradients were partially sintered into the substrate at temperatures between 1075 and 1200 °C, at which temperature all organic compounds were burned out, leaving nothing behind but a bare SiO_2 nanomorphology gradient.

Another approach to the deposition of nanometre-sized particles on a surface has been described by Roth et al.[95] who thermally evaporated gold onto polystyrene in a vacuum chamber to form a thin film. Since the polymer–metal interaction is much weaker than the metal–metal interaction, the gold atoms form clusters in a self-assembly process. The gradient in cluster density was induced by using a blocking mask to shadow parts of the substrate.

2.2.2. Electrochemical etching (Si). If silicon is used as an anode in an electrochemical etching process, its surface is rendered porous. The mean pore size and the size distribution can be adjusted by varying the HF concentration in the electrolyte and the current density on the anode. A current density gradient along the substrate can be achieved by suitable design of the electrodes, leading to a porosity gradient in the silicon wafer. Different configurations of electrodes and compositions of the HF solution have been used to create such gradients on boron-doped silicon substrates (p+). Collins et al.[96] placed an off-centre Pt cathode 1 mm above the substrates (1.2 cm diameter discs). The pore diameters in the gradients ranged from 600 nm immediately below the counter electrode to 10 nm on the side furthest away from it.
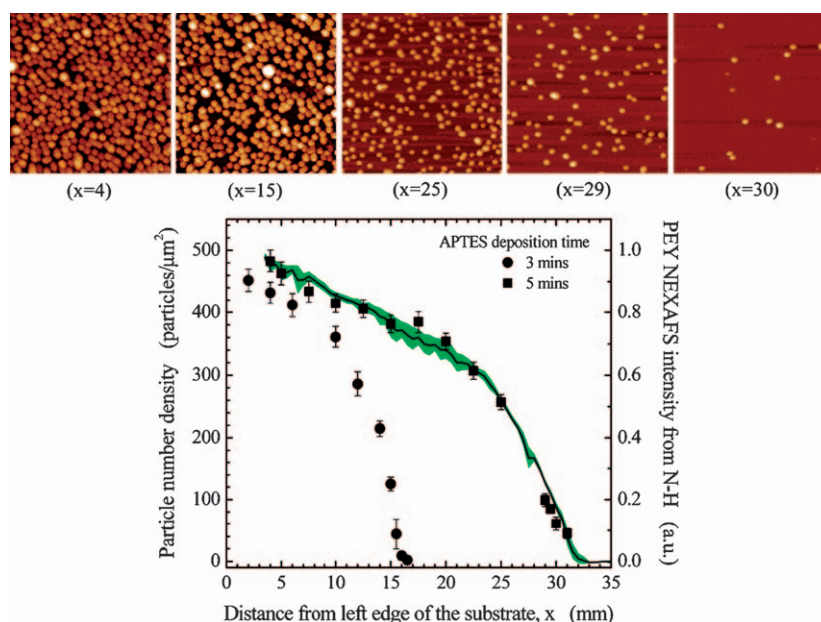

Fig. 7 (upper panel) AFM images of gold particles adsorbed along a substrate prepared by evaporating a mixture of (3-aminopropyl)triethoxysilane (APTES) and paraffin oil (PO) for 5 min followed by immersion in colloidal gold solution for 24 h (edge of each image = 1 μm). (lower panel) Particle number density profile (left) for two gradients prepared by evaporating APTES–PO mixtures for 3 and 5 min. The line represents the PEY NEXAFS profile (right) of N–H bonds from an ATEPS gradient prepared by evaporating the APTES–PO mixture for 5 min.[93]
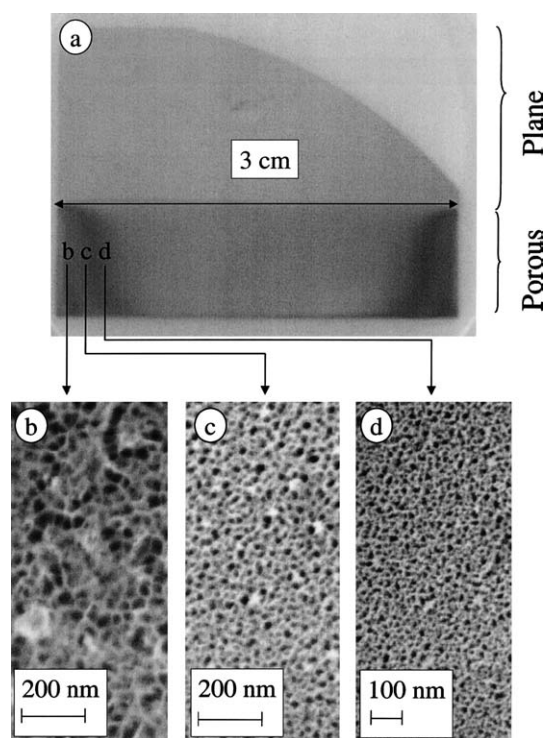
Fig. 8 (a) An etched porous silicon gradient. One gradient stretches from the left to the center and one from the right to the centre, as seen by the change in the gray scale. (b–d) SEM pictures taken of the wafer seen in (a) at different distances from the edge; (b) at the edge of the wafer (*i.e.*, 0 mm), (c) 2.5 mm from the edge of the wafer, and (d) 4 mm from the edge of the wafer.[97]

A different approach has been described by Karlsson *et al.*[97] They placed two similarly sized silicon wafers with their unpolished sides facing each other, separated by 2–15 cm. When applying a voltage between the wafers, the current density between them decreases from the edges towards the centre, yielding pore diameters in these gradients ranging from 20 nm to 3 nm from the edge to the centre (see Fig. 8).

2.2.3. Erosion/chemical polishing—replica methods. Another approach to the generation of morphological gradients is to gradually polish a rough surface. This was first described by Kunzler *et al.*,[98] who established a two-step process of particle erosion followed by chemical polishing. Pure aluminium sheets were sand-blasted with corundum particles and the substrate was subsequently fully immersed into the chemical polishing solution and then withdrawn in a controlled manner by means of a linear-motion drive, creating a roughness gradient on the centimetre scale (see Fig. 9a). A chemical-polishing solution was chosen that preferentially removed exposed features with a small radius of curvature. The composition of the polishing solution was 77.5% (v/v) phosphoric acid, 16.5% (v/v) sulfuric acid and 6% (v/v) nitric acid.

While aluminium is well suited to this approach, it may not be appropriate for a particular application. Also, it may be desirable to produce multiple identical samples for reproducibility reasons. These issues can be solved by replicating the gradients.[98] A negative impression can be made with a polyvinylsiloxane

replica material, which is widely used in dentistry. Subsequently an epoxy positive can be cast from the negative, creating a replica of the roughness gradient. These replicas can then be coated with metals or oxides, and these coatings can, in turn, be functionalised, providing great flexibility in the final surface chemistry of the morphology gradient.

2.2.4. Polymers—temperature gradient. Polymers are very versatile, displaying a wide range of properties, and thus many polymer-based approaches have been developed. A method introduced by Meredith *et al.*[99] is based on the phase separation of a polymer blend upon heating. Since the authors intended to create a two-dimensional gradient it was necessary to create a composition gradient perpendicular to the temperature gradient. A continuously changing composition of two polymers in solution was obtained by pumping one polymer into a solution of the other. Simultaneously the mixture was withdrawn into a syringe, which thereby became filled with a composition gradient that could subsequently be used to extrude a stripe of changing composition onto a silicon substrate. A knife-edge coater was then used to spread the stripe in a thin film with a gradually changing composition perpendicular to a temperature gradient, which in turn led to a gradual phase separation of the polymer blend. The result is a two-dimensional gradient of feature size and distribution. The same group used a similar coater to create thickness gradients of thin polymer films.[100] A bead of polymer solution was placed between the blade and the substrate, which was firmly mounted onto the stage. Then, the blade was constantly accelerated with respect to the substrate causing the frictional drag to increase and thus increasing the amount of polymer deposited on the substrate. After the solvent was evaporated, a thickness gradient remained, whose steepness is defined by the acceleration of the blade (with thicknesses ranging from 50 to 250 nm).

Washburn *et al.*[101] used a temperature gradient to induce varying crystallinity and thus a roughness gradient on the nanometre length-scale. They created a thin film of poly(L-lactic acid) (PLLA) on a silanised silicon wafer, which was annealed on a temperature gradient ranging from 44 to 100 °C. The RMS values achieved with this method ranged from 0.54 to 13 nm.

Quite a different approach was used by Lu *et al.*[102] They produced a porosity gradient in a film of low-density polyethylene (LDPE) on a silicon wafer. The LDPE was dissolved in xylene at 90 °C and then recrystallised by slowly lowering the temperature while stirring. A clean silicon wafer was then dipped into this suspension to create a porous polymer film. By annealing the substrate on a temperature gradient reaching from 0 °C to well above 107 °C (T_m of the LDPE used) the porosity gradually changes along the gradient (see Fig. 10).

2.2.5. Polymers—solvents, spincoating. Recently a method was reported by Blondiaux *et al.*[103] that takes advantage of the phase separation of an immiscible polymer blend thin film in the presence of a surface-energy gradient. The gradually changing surface energy induces the phases of the polymer blend to separate into different morphologies along the gradient.

As a polymer blend a (50 : 50) w/w mixture of poly(methylmethacrylate) (PMMA) and poly(2-vinylpyridine) (P2VP) dissolved in MEK was used. It was then spin coated onto the substrates.
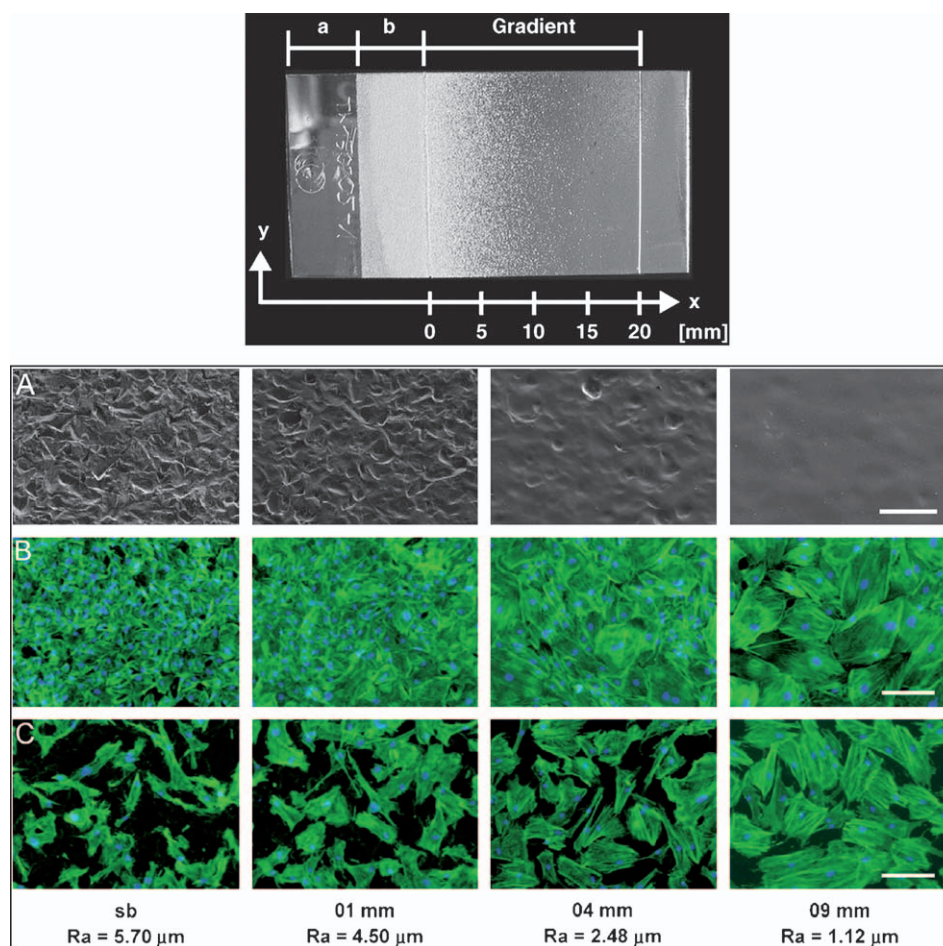
Fig. 9 (upper panel) Optical image of a roughness gradient on an aluminium surface over 20 mm. Section (a) shows the untreated aluminium surface and (b) a section that was sand blasted only.[98] (lower panel) (A) SEM images at different positions (sand blasted (sb), 1, 4 and 9 mm) and the corresponding roughness value Ra on a 10 mm roughness gradient of a similar type to that shown in Fig. 9a. Morphology of rat calvarial osteoblasts (B) and human gingival fibroblasts (C) at different positions on the gradient. Cells were cultured for 7 days. The nuclei were stained with DAPI (blue) and the actin network with Alexa Fluor 488 phalloidin (green). Scale bar is 200 μm.[117]

The morphology trend could be accentuated if one of the polymers was subsequently removed by means of a selective solvent.

2.2.6. Lithography. Photolithography can also be used to create morphological gradients on a surface. Rather than just creating a mask with gradually changing features, Cao *et al.*[104] used a regular photomask with uniform microfeatures. To create a gradient, an additional blocking mask was mounted just above the photoresist surface. While exposing the substrate, light diffraction occurs at the edge of the blocking mask, generating a gradient of light intensity on the low-contrast photoresist below. This leads to a gradient in dissolution by the developer that subsequently is transferred onto the Si substrate by reactive ion etching. The gradients created by these authors have been used to slowly narrow down the cross section in a fluidic channel, in order to allow long DNA molecules to be stretched so they can be inserted into nanochannels.

3. Applications

Chemical and morphological gradients have been used in a variety of applications, especially in the biomedical field and for studying wetting phenomena. These applications will be covered in more detail in the following section. In 1997 Ruardy *et al.* published a review[5] on the interaction of different types of proteins with wettability gradients, and a recent review by Genzer *et al.*[105] covers the use of polymer brush gradients for nanoparticle assembly and for studying protein adsorption.

3.1. Protein adsorption

Protein adsorption studies on gradient surfaces can be divided into roughly two categories. In the biomedical area one seeks to generate biocompatible implant surfaces to prevent foreign body response and facilitate the ingrowth of the implant. For this purpose it is important to understand the driving forces governing non-specific protein adsorption, for example on surfaces with different wettability, roughness or polymer-chain density. A different approach is needed for biosensors, where specific interactions, such as specific protein adsorption or antibody–antigen interactions are monitored.

Most of the early studies using surface gradients and proteins focused on their interaction with wettability gradients. The adsorption behaviour was found to vary for the same type of
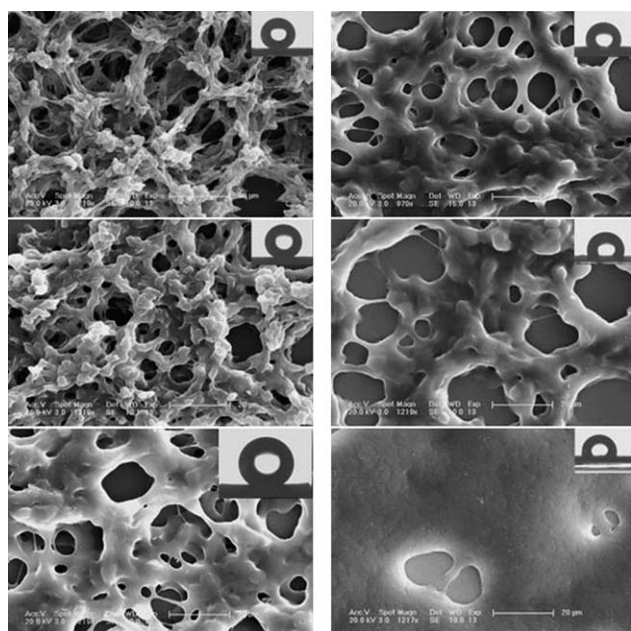
Fig. 10 FE-SEM micrographs of low-density polyethylene (LDPE) gradient surface along the major axis after processing in a temperature-gradient field. The micrographs correspond to the different location on the surface from low to high temperature. The insets are the corresponding profiles of a water drop on the surfaces.[102]

Fig. 11 Adsorption of pepsin and lysozyme onto a charge gradient prepared by alkanethiol cross-diffusion (C_{16}–NH_3^+–C_{15}–COO^-) studied by scanning ellipsometry. The adsorption time was 1.5 h, the concentration was 1 mg mL^{-1}, and the pH was 6.0.[38]

wettability gradient, depending on the adsorption conditions and the type of protein. The adsorption of fibrinogen and immunoglobulin G (IgG) was, for example, reduced when albumin was present in the solution due to the difference in adsorption kinetics between the proteins.[25] Surface wettability was also found to play a role in the Vroman effect.[106] While more human serum albumin (HSA), IgG, fibrinogen and lysozyme adsorbed on the hydrophobic end,[22,24,107,108] more human low-density lipoprotein (LDL) and high molecular weight kininogen was found to adsorb on the hydrophilic end.[22,109] This difference in adsorption behaviour can be attributed exclusively to the properties of the proteins. The following example, however, shows that this is not always the case. Spijker et al. reported more human serum albumin, fibrinogen and IgG adsorption on the hydrophilic end of a wettability gradient,[54] whereas Gölander et al. reported opposite behaviour.[25] The differences of the results in this case were attributed mainly to the different techniques used to prepare the gradients, and concomitantly to the different surface-chemical functionalities and the change in roughness. Similarly Loos et al. reported that the higher amount of enzyme (Candida antarctica lipase B) found on the hydrophilic end of a wettability gradient could not be attributed to the wettability alone, but was also influenced by surface roughness.[27] Not only the adsorption of proteins was studied, but also their desorption when exposed to nonionic detergents.[110] Welin-Klintström et al. compared wettability gradients prepared by two different methods and found that for one type of gradient not only the hydrophilicity but also the amount of negatively charged groups increased towards one end.[7] This additional effect was found to influence fibrinogen adsorption, which was higher on the charged surface. Finally, Riepl et al. have not only gradually varied surface wettability but also surface
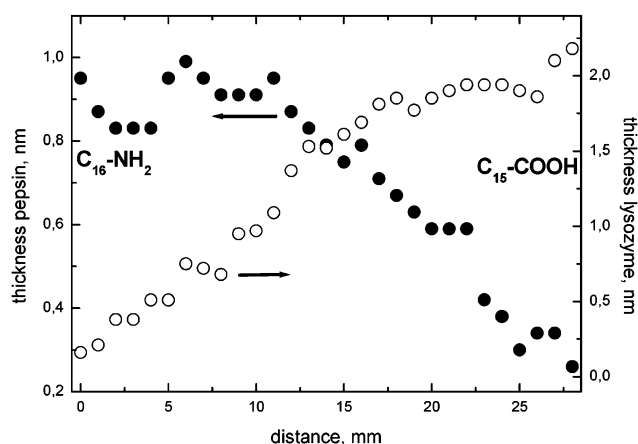
charge.[38] These charge gradients allowed the separation of lysozyme and pepsin protein mixtures, since the negatively charged pepsin adsorbs with higher probability onto the positively charged end, whereas the positively charged lysozyme behaves in the opposite way (see Fig. 11).

Riepl et al. have also used oligo(ethylene glycol) modified surfaces to study fibrinogen adsorption.[38] They found that the conformation of short oligo(ethylene glycol) chains controls protein adsorption. A helical chain conformation appeared to be resistant towards non-specific fibrinogen adsorption, whereas an all-trans orientation allowed protein adsorption. Brush-like poly(ethylene glycol) (PEG) coatings have been shown to render surfaces resistant towards non-specific protein adsorption.[111] PEG surface-density gradients have also been used to monitor protein adsorption.[57,64,70] Less protein (human serum albumin, IgG, fibrinogen, human serum and human plasma protein) was found to adsorb at the high-density end, as expected from studies with homogeneously covered substrates. Lin et al. reported contradictory results, where more fibrinogen was found to adsorb on the high PEG-chain density. However, this behaviour was exceptional and was attributed to interactions with additional, charged groups on the surface. Additionally, it has been shown that depending on the shape and size of the protein, different PEG densities are needed to reach a similar level of protein resistance.[70] Also, shorter PEG chains are less effective at reducing human plasma protein adsorption.[64] Other brush-like polymer coatings with gradually changing surface density, such as gradients from poly(2-hydroxyethylmethacrylate) (HEMA),[33,112] and poly(ω-methacryloyloxyalkylphosphoryl-choline) (MAPC)[59] have also been used to gradually reduce fibronectin adsorption with increasing chain density.

The adsorption of proteins onto morphological gradients has not yet been studied extensively. Collins et al.[96] and Karlsson et al.[97] both reported a higher albumin adsorption at the highly porous end of a morphology gradient, than at the gradient end with smaller pore sizes. However, the adsorption behaviour could not solely be attributed to the change in pore size, since the total thickness of the layer and the chemistry may also change with position.
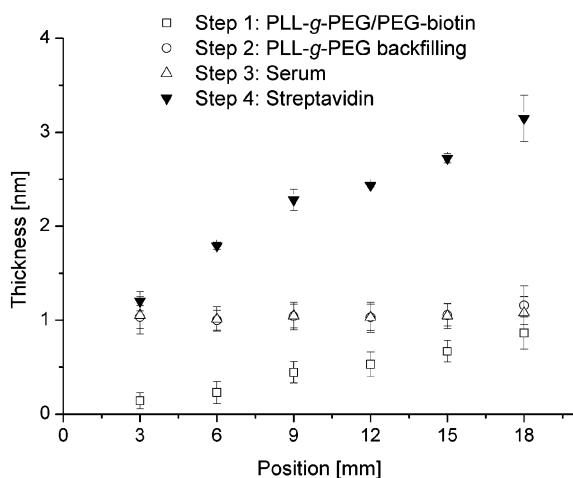
Fig. 12 Ellipsometric adlayer thickness of a biotinylated gradient as a function of the gradient position. A biotinylated coverage gradient was generated (step 1, linear increase in thickness), which was then back-filled with unmodified PLL-*g*-PEG (step 2, constant layer thickness). Negligible serum adsorption was found on such a functionalised gradient (step 3, no notable increase in layer thickness), while the amount of immobilised streptavidin gradually increased along the gradient (step 4, increasing thickness with increasing biotin density).[70]

Gradients have also been prepared directly from immunoglobulin G (IgG) by gradual immobilisation.[79,89] The efficiency of the antibody–antigen interaction on such IgG density gradients depends on the antigen surface density. An optimum surface density was found for both types of gradient. Steric hindrance and the confined space on the surface seem to prevent an efficient interaction at high antigen surface densities. Finally, biotin has also been gradually immobilised onto other gradients: streptavidin adsorption was found to reach saturation at a certain biotin density on a biotin gradient prepared by adsorption onto a wettability gradient.[60] Biotin gradients were also prepared by the saturation of a PEG-chain density gradient with a functionalised (biotinylated) brush-copolymer.[70] Fig. 12 shows that streptavidin binds gradually onto such substrates (step 4), whereas no unspecific serum adsorption occurs (step 3).

3.2. Cell adhesion

The adhesion of cells is important in many biomedical applications, for example for hip or dental root implants. A successful integration of these implants requires that bone cells adhere to the implant surface and proliferate. It is therefore important to understand the adhesion and proliferation of cells on surfaces with different properties, *e.g.* wettability or roughness. Different types of gradients, wettability, polymer-chain density, protein and morphology gradients, have therefore been used to study cell adhesion.

Depending on the type of cells and the presence of proteins in the solution, the adhesion of cells to wettability gradients has been observed to vary. Whereas endothelial cells adsorb, proliferate and grow more pronouncedly on the hydrophobic end of wettability gradients,[3] algal spores behave differently and adhere more strongly to the hydrophilic end.[113] On the other hand,

Kennedy *et al.* found similar osteoblast adhesion along the entire wettability gradient, although more pronounced proliferation was observed at the hydrophobic end.[29] Finally, Lee *et al.* reported increased pheochromocytoma cell (PC-12) adhesion to an intermediate surface wettability, whereas neurite growth was enhanced at the hydrophilic end.[9] The results of all these studies, however, are influenced by the presence of proteins and other components in the cell media, which may pre-adsorb onto the wettability gradient and mediate cell adhesion, especially in those cases where enhanced cell adhesion corresponds to an enhanced protein adsorption.[9]

A more consistent picture is found for cells adhering to gradients in polymer-chain density. The protein-resistant coatings provided by high-density polyHEMA, polyMAPC, PEG coatings correspond to non-adhesive regions for cells. This means that fibronectin, as well as fibroblasts,[33,59] and osteoblasts[112] preferentially adhere to the low-density end of the gradients. Mougin *et al.* also found that the adhesion of endothelial cells was decelerated at the low-density end.[67] Not only the cells themselves, but also cell fragments, such as blood platelets, were found to adhere increasingly to the low PEG density end of a gradient.[64] Finally, a PEG-chain density gradient was back-filled with kinesin, a motor protein, which allows microtubules to be sorted according to their length[73] (see Fig. 13).

Since cell adhesion depends on the presence of certain proteins on a surface, protein density gradients have also been prepared and tested. Bovine serum albumin (BSA) is known to decrease cell adhesion, while other proteins, for example fibronectin, enhance the interaction. A fibronectin concentration gradient saturated with BSA leads to the selective adhesion of fibroblasts to the fibronectin-coated regions[81] (Fig. 14) and to endothelial
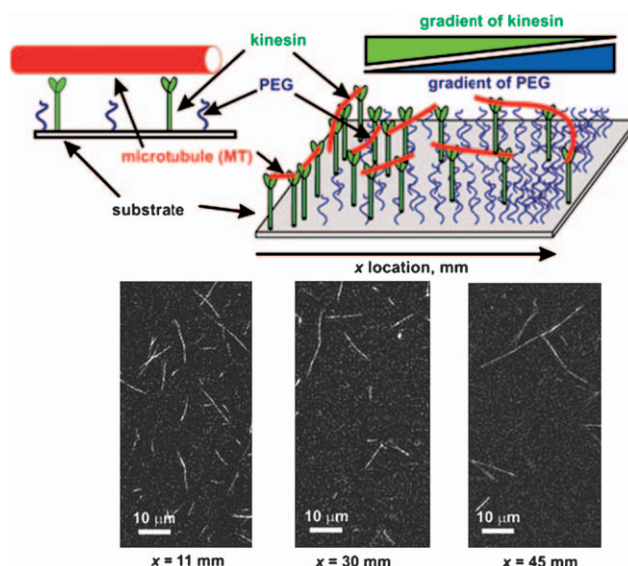

Fig. 13 Gliding motility of microtubules on a poly(ethylene glycol) (PEG)-gradient surface with immobilised kinesin. Upper part: schematic diagram of the motility system. Although the grafting density of PEG increases from left to right, the kinesin gradient is formed in the opposite direction. Lower part: fluorescence micrographs of gliding microtubules taken at three different locations along the gradient surface. At lower kinesin density, the number of microtubules per field of view decreases, whereas the average length of the microtubules increases.[73]
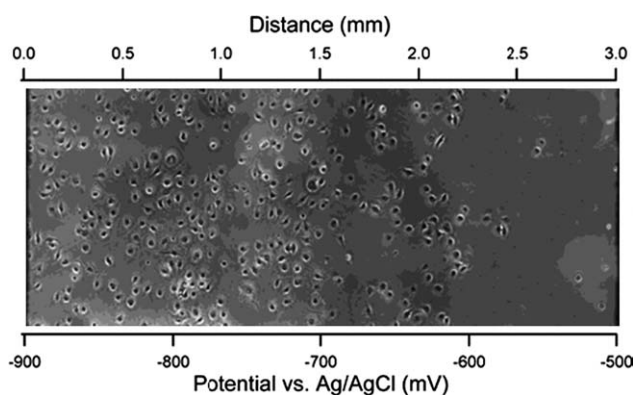
Fig. 14 Optical micrograph showing the adhesion of 3T3 fibroblast cells on a MUA–MUD-derived FN–BSA gradient prepared by electrochemical desorption. The top and bottom *x*-axes show the spatial/potential distribution of the cells.[81]

cell migration towards higher fibronectin densities.[37] The cell migration and directedness of endothelial cells was also found to increase with a higher laminin density.[8] Several protein gradients, *e.g.* laminin concentration gradients, were employed to direct the outgrowth of axons into the direction of a higher protein concentration, mimicking axon outgrowth in nature[83,114,115] (see Fig. 15).

Not only surface chemistry but also surface roughness is known to influence cell adhesion and proliferation.[116] Two different ranges of surface roughness gradients have been tested, on the one hand roughness gradients with microfeatures (see Fig. 9b), on the other hand gradients with a roughness change on the nanoscale (Fig. 16). Osteoblasts exhibited a different
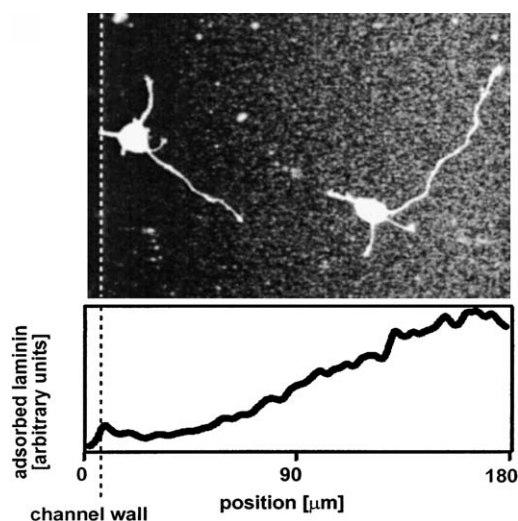

Fig. 15 Fluorescence micrograph of rat hippocampal neurons preferentially extending their presumptive axon (their longest process) in the direction of increasing surface density of laminin. Neurons were fixed after 24 h in culture and immunostained for laminin (to visualise the substrate-bound gradient in laminin) and tubulin (to picture the microtubules of the neurons). The shape of the immobilised gradient in laminin is shown in the graph below the micrograph. The dotted line indicates the left wall of the channel.[114]

behaviour on the two types of gradients. Whereas proliferation increased towards a higher surface roughness on the micrometre scale,[117] the opposite behaviour was found for nanofeature gradients.[101,118] In order to adhere to surfaces, cells need to form focal contacts. The spacing between particles is in the nanometre range, meaning much smaller than the size of the cells. If the spacing between particles is small, the cells need to deform their membrane substantially in order to attach. This unfavorable deformation leads to a decreased cell adhesion. Meredith *et al.* also found osteoblast adhesion and differentiation to differ on gradients with varying chemistry, microstructure and roughness.[99] Fibroblasts were not yet tested on both types of gradients, but contradictory behaviour was found on the micrometre scale. There, fibroblasts showed the opposite proliferation behaviour with the proliferation decreasing with increasing roughness.[117]

Finally, specific peptide sequences have also been gradually immobilised on surfaces, since certain peptide sequences are thought to trigger cell adhesion. Two gradient studies have confirmed this view, Herbert *et al.* having found an enhanced fibroblast adhesion on the high-peptide-density end,[119] and smooth muscle cells (SMC) also having displayed increased adhesion[30] (Fig. 17a–c).

3.3. Wettability effects

Wettability gradients are the ideal tool for studying various effects related to changing surface energy, such as superhydrophobicity or the movement of small water droplets.

In 1992 Chaudhury and Whitesides reported the movement of a water droplet along a 1 cm long wettability gradient, prepared by silane vapour diffusion[13] (Fig. 18). They demonstrated that a microlitre droplet will move along a wettability gradient, and even on an inclined surface, if the contact-angle hysteresis on the surface is small (<10°). The movement of droplets along wettability gradients was further studied in detail by Daniel *et al.*[13,15,120] They reported that the droplet movement is driven by the unbalanced contact angles at the droplet edges in the direction of the gradient. The contact-angle hysteresis could be overcome by vibration, thus causing droplet motion also on surfaces with higher contact-angle hysteresis.[15] They studied the influence of the amplitude and frequency of the vibration in detail and the influence of the viscosity of the liquid on the velocity of the drop. Several groups have also presented theoretical considerations concerning droplet movement and the prediction of droplet speed, and have compared the different models with experimental results.[17,121,122] Petrie *et al.* showed that the velocity of the droplet can not only be increased by reducing the surface hysteresis, but also by reducing friction through the combination of an etched porous silica surface and fluorinated silane SAMs.[21] Droplet movement was also studied in order to characterise the surface wettability by Choi and Newby, who combined polymer dewetting with droplet movement and extracted surface tension values.[26] Not only the movement of microlitre droplets, but also the condensation of very small droplets was observed on wettability gradients. Zhao and Beysens found no directed movement of such small droplets, but a different growth behaviour at the ends of the gradients.[16] With a growing droplet size, they observed that the centre of gravity of the droplet moved towards the more hydrophilic end of the gradient.
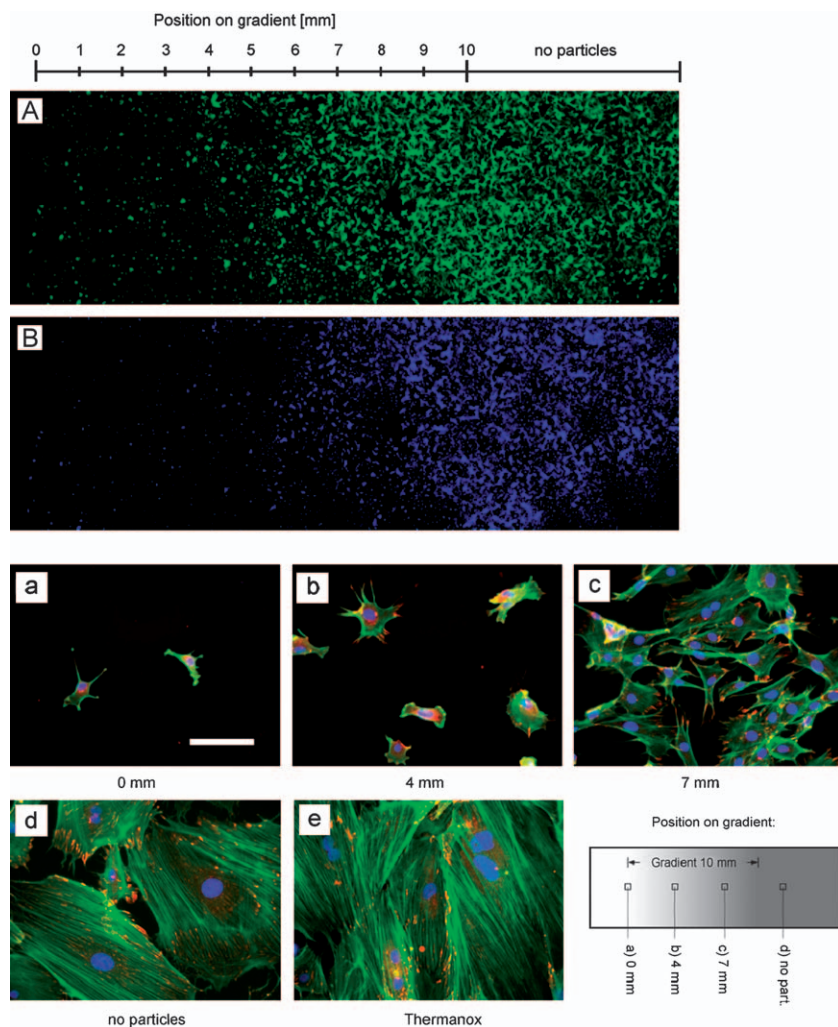
Fig. 16 (a) Fluorescence images of RCO on a nanoparticle-density gradient. Images show an overview of a large part of the gradient. Cells were seeded at a density of 3500 cells cm^{-2} and cultured for 7 days. After fixation, cells were stained with FITC for actin (green) and with DAPI for the nuclei (blue). (b) Fluorescence images of cell morphology at different positions on a nanoparticle-density gradient. RCOs were seeded at a density of 3500 cells cm^{-2} and cultured for 7 days. After fixation cells were stained for vinculin (red), actin (green) and the nuclei (blue). With decreasing particle density, cells formed well-constituted focal adhesions (red) and a distinctive actin network (green). Image e is the Thermanox control surface. Scale bar is 100 μm.[118]

Superhydrophobicity is an increasingly studied phenomenon since the easy generation of superhydrophobic surfaces would open up many new possibilities for industrial applications. Several groups have combined rough surfaces with a chemical gradient.[32,123] In this way they managed to create surfaces with a superhydrophilic to superhydrophobic transition with a high hysteresis. Lu *et al.* did not vary the chemistry, but only the surface topography in a gradual way and managed to generate a transition from superhydrophobic to hydrophobic (150° to 97°).[102]

Finally, composition gradients from two different polymer chains have also been used to study wettability effects. A polystyrene–poly(2-vinylpyridine) gradient allows a switchable wettability if submitted to a selective solvent treatment.[71] In the selective solvent, one of the two chains collapses and the properties of the surface are determined by mainly the other component. The same effect can be exploited when submitting a polyelectrolyte gradient (poly(*tert*-butylacrylate) *vs.* poly(2-vinylpyridine)) to a pH change,[72] Fig. 19.

3.4. Other applications

Surface chemical and morphological gradients have also been used for several other purposes, ranging from the study of fundamental phenomena to industrial applications.

Several chemical gradients have been used to carry out fundamental studies. Wu *et al.* have observed the mushroom-to-brush transition in polymer brush gradients,[55] while Genzer *et al.* studied the formation mechanism and structure of silane SAMs.[10] They found that the formation mechanism depends strongly on the type of head group and the humidity. Also two-component polymer brush gradients were submitted to a selective solvent treatment, which allowed the creation of a roughness gradient due to the collapse of one type of polymer chains.[56]

Gradients also simplify the development of new analytical techniques, as shown by Bhat *et al.*, since they allow the testing of very different surface compositions under the same environmental conditions, thus minimising the experimental error.[63]
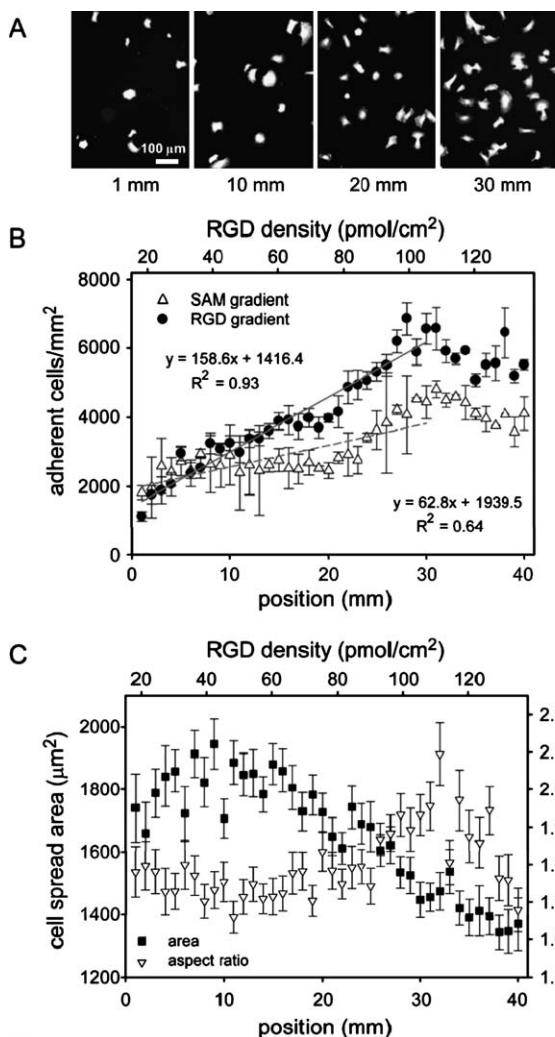
Fig. 17 Cell adhesion and morphology vary with surface-conjugated RGD peptide density. A) Cells were fluorescently labeled, and cell numbers, areas and aspect ratios quantified. B) The number of cells adhering to SAM ($\triangle$) or RGD ($\bullet$) conjugated gradients increases with position. A second axis (top) was added to indicate cell adhesion as a function of approximate RGD density. C) Cell areas ($\blacksquare$) and aspect ratios ($\blacklozenge$, mean $\pm$ S.E., $n > 45$) *versus* position and RGD concentration (top axis, derived from linear regression in Fig. 2) show different trends.[30]

Fig. 18 Uphill motion of a drop of water on a gradient surface. The gradient surface was inclined by <15° from the horizontal plane. The volume of the drop was <1 µl. The moving drop was photographed with an automatic camera that exposed one frame every 0.4 s. The drop moved more rapidly on the initial part of the gradient than on the final part.[13]

A recent area of interest also lies in the field of liquid crystal displays (LCDs). Almost all liquid crystal devices rely on the control of liquid crystal orientation at the device interface. Surface-chemical gradients are a useful tool to study the alignment of LCs, since they facilitate the study of the systematic change in orientation from homeotropic to planar. Gradient studies have revealed that several factors seem to influence this change in orientation, for example the wettability of the surface, the thickness of the liquid crystal device[124] or the arrangement and tilt angle of the underlying anchoring layer.[125]

Surface-chemical as well as -morphological gradients have been used to study the adhesion of thin polymeric films. Chiang *et al.* carried out delamination tests on an orthogonal wettability *vs.* thickness gradient. They found that the delamination of the polymer film with increasing temperature depends on both
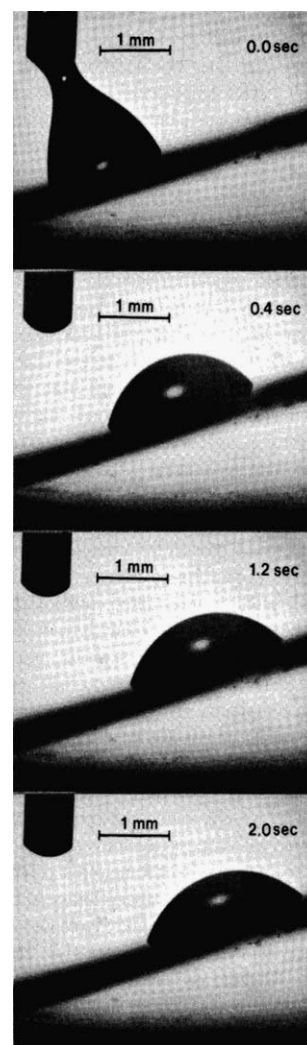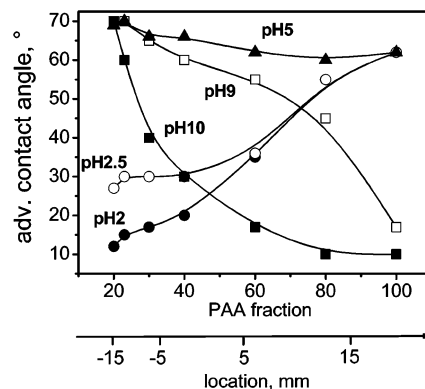

Fig. 19 Switching of the water contact angle of the gradient PAA-*mix*-PVP brush *vs.* composition (upper *X*-axis) and location of the probing drop on the sample (lower *X*-axis) upon exposure to water of different pHs (($\bullet$) pH = 2, ($\circ$) pH = 2.5, ($\blacktriangle$) pH = 5, ($\square$) pH = 9, ($\blacksquare$) pH = 10).[72]

parameters.[126] The generation of such combined libraries allows the rapid screening of optimal surface parameters for different applications. Preliminary peel tests carried out in our laboratory have shown that not only the surface chemistry, but also the surface roughness can be explored in a high-throughput way on a gradient.[127] Tests with commercially available tape showed that the adhesion increases with surface roughness, although it also depends on the viscoelastic properties and thickness of the glue film. Morphology gradients have also been used to align DNA molecules.[104]

Finally, many other applications can also be envisaged, including optimising the surface chemistry for sensors, filters, or catalysts, as well as the use of gradients as templates for further experiments, such as the growth of nanostructures or crystals or for fundamental studies in tribology.

References

1   J. H. Lee, H. G. Kim, G. S. Khang, H. B. Lee and M. S. Jhon, *J. Colloid Interface Sci.*, 1992, **151**, 563–570.
2   W. G. Pitt, *J. Colloid Interface Sci.*, 1989, **133**, 223–227.
3   T. Uedayukoshi and T. Matsuda, *Langmuir*, 1995, **11**, 4135–4140.
4   H. Elwing and C. G. Golander, *Adv. Colloid Interface Sci.*, 1990, **32**, 317–339.
5   T. G. Ruardy, J. M. Schakenraad, H. C. vanderMei and H. J. Busscher, *Surf. Sci. Rep.*, 1997, **29**, 3–30.
6   V. Hlady and C. H. Ho, *Materialwiss. Werkstofftech.*, 2001, **32**, 185–192.
7   S. Welin-Klintstrom, M. Lestelius, B. Liedberg and P. Tengvall, *Colloids Surf., B*, 1999, **15**, 81–87.
8   R. C. Gunawan, J. Silvestre, H. R. Gaskins, P. J. A. Kenis and D. E. Leckband, *Langmuir*, 2006, **22**, 4250–4258.
9   S. J. Lee, G. Khang, Y. M. Lee and H. B. Lee, *J. Colloid Interface Sci.*, 2003, **259**, 228–235.
10 J. Genzer, K. Efimenko and D. A. Fischer, *Langmuir*, 2006, **22**, 8532–8541.
11 R. A. Potyrailo and L. Hassib, *Rev. Sci. Instrum.*, 2005, **76**, 062225.
12 M. B. J. Wijesundara, E. Fuoco and L. Hanley, *Langmuir*, 2001, **17**, 5721–5726.
13 M. K. Chaudhury and G. M. Whitesides, *Science*, 1992, **256**, 1539–1541.
14 S. Daniel, M. K. Chaudhury and J. C. Chen, *Science*, 2001, **291**, 633–636.
15 S. Daniel and M. K. Chaudhury, *Langmuir*, 2002, **18**, 3404–3407.
16 H. Zhao and D. Beysens, *Langmuir*, 1995, **11**, 627–634.
17 H. Suda and S. Yamada, *Langmuir*, 2003, **19**, 529–531.
18 J. Genzer, *J. Adhes.*, 2005, **81**, 417–435.
19 K. Efimenko and J. Genzer, *Adv. Mater.*, 2001, **13**, 1560.
20 J. Genzer, D. A. Fischer and K. Efimenko, *Adv. Mater.*, 2003, **15**, 1545.
21 R. J. Petrie, T. Bailey, C. B. Gorman and J. Genzer, *Langmuir*, 2004, **20**, 9893–9896.
22 H. Elwing, S. Welin, A. Askendal, U. Nilsson and I. Lundstrom, *J. Colloid Interface Sci.*, 1987, **119**, 203–210.
23 L. M. A. Vandesteeg and C. G. Golander, *Colloids Surf.*, 1991, **55**, 105–119.
24 V. Hlady, *Appl. Spectrosc.*, 1991, **45**, 246–252.
25 C. G. Golander, Y. S. Lin, V. Hlady and J. D. Andrade, *Colloids Surf.*, 1990, **49**, 289–302.
26 S. H. Choi and B. M. Z. Newby, *Langmuir*, 2003, **19**, 7427–7435.
27 K. Loos, S. B. Kennedy, N. Eidelman, Y. Tai, M. Zharnikov, E. J. Amis, A. Ulman and R. A. Gross, *Langmuir*, 2005, **21**, 5237–5241.
28 S. V. Roberson, A. J. Fahey, A. Sehgal and A. Karim, *Appl. Surf. Sci.*, 2002, **200**, 150–164.
29 S. B. Kennedy, N. R. Washburn, C. G. Simon and E. J. Amis, *Biomaterials*, 2006, **27**, 3817–3824.
30 N. D. Gallant, K. A. Lavery, E. J. Amis and M. L. Becker, *Adv. Mater.*, 2007, **19**, 965–969.
31 Y. Ito, M. Heydari, A. Hashimoto, T. Konno, A. Hirasawa, S. Hori, K. Kurita and A. Nakajima, *Langmuir*, 2007, **23**, 1845–1850.
32 J. T. Han, S. Kim and A. Karim, *Langmuir*, 2007, **23**, 2608–2614.
33 Y. Mei, T. Wu, C. Xu, K. J. Langenbach, J. T. Elliott, B. D. Vogt, K. L. Beers, E. J. Amis and N. R. Washburn, *Langmuir*, 2005, **21**, 12309–12314.
34 B. Liedberg and P. Tengvall, *Langmuir*, 1995, **11**, 3821–3827.
35 B. Liedberg, M. Wirde, Y. T. Tao, P. Tengvall and U. Gelius, *Langmuir*, 1997, **13**, 5329–5334.
36 M. Lestelius, I. Engquist, P. Tengvall, M. K. Chaudhury and B. Liedberg, *Colloids Surf., B*, 1999, **15**, 57–70.
37 J. T. Smith, J. K. Tomfohr, M. C. Wells, T. P. Beebe, T. B. Kepler and W. M. Reichert, *Langmuir*, 2004, **20**, 8279–8286.
38 M. Riepl, M. Ostblom, I. Lundstrom, S. C. T. Svensson, A. W. D. van der Gon, M. Schaferling and B. Liedberg, *Langmuir*, 2005, **21**, 1042–1050.
39 R. H. Terrill, K. M. Balss, Y. M. Zhang and P. W. Bohn, *J. Am. Chem. Soc.*, 2000, **122**, 988–989.
40 Q. Wang, J. A. Jakubowski, J. V. Sweedler and P. W. Bohn, *Anal. Chem.*, 2004, **76**, 1–8.
41 S. T. Plummer and P. W. Bohn, *Langmuir*, 2002, **18**, 4142–4149.
42 K. M. Balss, G. A. Fried and P. W. Bohn, *J. Electrochem. Soc.*, 2002, **149**, C450–C455.
43 R. R. Fuierer, R. L. Carroll, D. L. Feldheim and C. B. Gorman, *Adv. Mater.*, 2002, **14**, 154–157.
44 N. Blondiaux, S. Zurcher, M. Liley and N. D. Spencer, *Langmuir*, 2007, **23**, 3489–3494.
45 N. Ballav, A. Shaporenko, A. Terfort and M. Zharnikov, *Adv. Mater.*, 2007, **19**, 998–1000.
46 R. Klauser, C. H. Chen, M. L. Huang, S. C. Wang, T. J. Chuang and M. Zharnikov, *J. Electron Spectrosc. Relat. Phenom.*, 2005, **144**, 393–396.
47 T. Kraus, R. Stutz, T. E. Balmer, H. Schmid, L. Malaquin, N. D. Spencer and H. Wolf, *Langmuir*, 2005, **21**, 7796–7804.
48 M. Geissler, P. Chalsani, N. S. Cameron and T. Veres, *Small*, 2006, **2**, 760–765.
49 L. Pardo, W. C. Wilson and T. J. Boland, *Langmuir*, 2003, **19**, 1462–1466.
50 A. Y. Sankhe, B. D. Booth, N. J. Wiker and S. M. Kilbey, *Langmuir*, 2005, **21**, 5332–5336.
51 S. Morgenthaler, S. Lee, S. Zürcher and N. D. Spencer, *Langmuir*, 2003, **19**, 10459–10462.
52 S. Morgenthaler, S. Lee and N. D. Spencer, *Langmuir*, 2006, **22**, 2706–2711.
53 N. V. Venkataraman, S. Zürcher and N. D. Spencer, *Langmuir*, 2006, **22**, 4184–4189.
54 H. T. Spijker, R. Bos, W. van Oeveren, J. de Vries and H. Busscher, *Colloids Surf., B*, 1999, **15**, 89–97.
55 T. Wu, K. Efimenko and J. Genzer, *J. Am. Chem. Soc.*, 2002, **124**, 9394–9395.
56 B. Zhao, *Langmuir*, 2004, **20**, 11748–11755.
57 Y. S. Lin, V. Hlady and C. Golander, *Colloids Surf., B*, 1994, **3**, 49–62.
58 B. J. Jeong, J. H. Lee and H. B. Lee, *J. Colloid Interface Sci.*, 1996, **178**, 757–763.
59 Y. Iwasaki, S. Sawada, N. Nakabayashi, G. Khang, H. B. Lee and K. Ishihara, *Biomaterials*, 1999, **20**, 2185–2191.
60 M. S. Kim, K. S. Seo, G. Khang and H. B. Lee, *Langmuir*, 2005, **21**, 4066–4070.
61 J. H. Lee, H. W. Kim, P. K. Pak and H. B. Lee, *J. Polym. Sci., Part A: Polym. Chem.*, 1994, **32**, 1569–1579.
62 R. R. Bhat, J. Genzer, B. N. Chaney, H. W. Sugg and A. Liebmann-Vinson, *Nanotechnology*, 2003, **14**, 1145–1152.
63 R. R. Bhat, M. R. Tomlinson and J. Genzer, *J. Polym. Sci., Part B: Polym. Phys.*, 2005, **43**, 3384–3394.
64 J. H. Lee, B. J. Jeong and H. B. Lee, *J. Biomed. Mater. Res.*, 1997, **34**, 105–114.
65 M. R. Tomlinson and J. Genzer, *Macromolecules*, 2003, **36**, 3449–3451.
66 M. R. Tomlinson and J. Genzer, *Langmuir*, 2005, **21**, 11552–11555.
67 K. Mougin, A. S. Ham, M. B. Lawrence, E. J. Fernandez and A. C. Hillier, *Langmuir*, 2005, **21**, 4809–4812.
68 C. Xu, T. Wu, C. M. Drain, J. D. Batteas and K. L. Beers, *Macromolecules*, 2005, **38**, 6–8.
69 A. Larsson and B. Liedberg, *Langmuir*, 2007, **23**, 11319–11325.

70 S. Morgenthaler, C. Zink, B. Städler, J. Vörös, S. Lee, N. D. Spencer and S. G. P. Tosatti, *Biointerphases*, 2006, **1**, 156–165.

71 L. Ionov, A. Sidorenko, M. Stamm, S. Minko, B. Zdyrko, V. Klep and I. Luzinov, *Macromolecules*, 2004, **37**, 7421–7423.

72 L. Ionov, N. Houbenov, A. Sidorenko, M. Stamm, I. Luzinov and S. Minko, *Langmuir*, 2004, **20**, 9916–9919.

73 L. Ionov, M. Stamm and S. Diez, *Nano Lett.*, 2005, **5**, 1910–1914.

74 X. J. Wang and P. W. Bohn, *Adv. Mater.*, 2007, **19**, 515–520.

75 C. Xu, S. E. Barnes, T. Wu, D. A. Fischer, D. M. DeLongchamp, J. D. Batteas and K. L. Beers, *Adv. Mater.*, 2006, **18**, 1427–1430.

76 J. D. Whittle, D. Barton, M. R. Alexander and R. D. Short, *Chem. Commun.*, 2003, **14**, 1766–1767.

77 B. P. Harris and A. T. Metters, *Macromolecules*, 2006, **39**, 2764–2772.

78 C. L. Hypolite, T. L. McLernon, D. N. Adams, K. E. Chapman, C. B. Herbert, C. C. Huang, M. D. Distefano and W. S. Hu, *Bioconjugate Chem.*, 1997, **8**, 658–663.

79 I. Caelen, H. Gao and H. Sigrist, *Langmuir*, 2002, **18**, 2463–2467.

80 X. J. Wang and P. W. Bohn, *J. Am. Chem. Soc.*, 2004, **126**, 6825–6832.

81 S. T. Plummer, Q. Wang, P. W. Bohn, R. Stockton and M. A. Schwartz, *Langmuir*, 2003, **19**, 7528–7536.

82 R. A. Venkateswar, D. W. Branch and B. C. Wheeler, *Biomed. Microdevices*, 2000, **2**, 255–264.

83 H. Baier and F. Bonhoeffer, *Science*, 1992, **255**, 472–475.

84 S. Kramer, H. Xie, J. Gaff, J. R. Williamson, A. G. Tkachenko, N. Nouri, D. A. Feldheim and D. L. Feldheim, *J. Am. Chem. Soc.*, 2004, **126**, 5388–5395.

85 S. H. Park and U. Krull, *Anal. Chim. Acta*, 2006, **564**, 133–140.

86 N. L. Jeon, S. K. W. Dertinger, D. T. Chiu, I. S. Choi, A. D. Stroock and G. M. Whitesides, *Langmuir*, 2000, **16**, 8311–8316.

87 S. K. W. Dertinger, D. T. Chiu, N. L. Jeon and G. M. Whitesides, *Anal. Chem.*, 2001, **73**, 1240–1246.

88 X. Y. Jiang, Q. B. Xu, S. K. W. Dertinger, A. D. Stroock, T. M. Fu and G. M. Whitesides, *Anal. Chem.*, 2005, **77**, 2338–2347.

89 I. Caelen, A. Bernard, D. Juncker, B. Michel, H. Heinzelmann and E. Delamarche, *Langmuir*, 2000, **16**, 9125–9130.

90 K. A. Fosser and R. G. Nuzzo, *Anal. Chem.*, 2003, **75**, 5775–5782.

91 R. R. Bhat and J. Genzer, *Appl. Surf. Sci.*, 2006, **252**, 2549–2554.

92 R. R. Bhat and J. Genzer, *Surf. Sci.*, 2005, **596**, 187–196.

93 R. R. Bhat, D. A. Fischer and J. Genzer, *Langmuir*, 2002, **18**, 5640–5643.

94 C. Huwiler, T. P. Künzler, M. Textor, J. Vörös and N. D. Spencer, *Langmuir*, 2007, **23**, 5929–5935.

95 S. V. Roth, M. Burghammer, C. Rieckel, P. Müller-Bauschbaum, A. Diethert, P. Panagiotou and H. Walter, *Appl. Phys. Lett.*, 2003, **82**, 1935.

96 B. E. Collins, K. S. Dancil, G. Abbi and M. J. Sailor, *Adv. Funct. Mater.*, 2002, **12**, 187–191.

97 L. M. Karlsson, P. Tengval, I. Lundström and H. Arwin, *J. Electrochem. Soc.*, 2002, **149**, C648–C652.

98 T. P. Kunzler, T. Drobek, C. M. Sprecher, M. Schuler and N. D. Spencer, *Appl. Surf. Sci.*, 2006, **253**, 2148–2153.

99 J. C. Meredith, J. L. Sormana, B. G. Keselowsky, A. J. Garcia, A. Tona, A. Karim and E. J. Amis, *J. Biomed. Mater. Res.*, 2003, **66A**, 483.

100 C. M. Stafford, K. E. Roskov, T. H. Epps III and M. J. Fasolka, *Rev. Sci. Instrum.*, 2006, **77**, 23908.

101 N. R. Washburn, K. M. Yamada, C. G. Simon Jr, S. B. Kennedy and E. J. Amis, *Biomaterials*, 2004, **25**, 1215.

102 X. Lu, J. Zhang, C. Zhang and Y. Han, *Macromol. Rapid Commun.*, 2005, **26**, 637.

103 N. Blondiaux, PhD thesis, No. 16699, ETH Zurich, 2006.

104 H. Cao, J. O. Tegenfeldt, R. H. Austin and S. Y. Chou, *Appl. Phys. Lett.*, 2002, **81**, 3058–3060.

105 R. R. Bhat, M. R. Tomlinson, T. Wu and J. Genzer, *Adv. Polym. Sci.*, 2006, **198**, 51–124.

106 H. Elwing, A. Askendal and I. Lundstrom, *J. Biomed. Mater. Res.*, 1987, **21**, 1023–1028.

107 Y.-S. Lin and V. Hlady, *Colloids Surf., B*, 1994, **2**, 481–491.

108 H. Elwing, S. Welin, A. Askendahl and I. Lundstrom, *J. Colloid Interface Sci.*, 1988, **123**, 306–308.

109 P. Tengvall, A. Askendal, I. Lundstrom and H. Elwing, *Biomaterials*, 1992, **13**, 367–374.

110 H. Elwing, A. Askendal and I. Lundstrom, *J. Colloid Interface Sci.*, 1989, **128**, 296–300.

111 J. M. Harris, *Poly(ethylene glycol) Chemistry and Biological Applications*, American Chemical Society, Washington, DC, 1997, vol. 680.

112 R. R. Bhat, B. N. Chaney, J. Rowley, A. Liebmann-Vinson and J. Genzer, *Adv. Mater.*, 2005, **17**, 2802–2807.

113 M. K. Chaudhury, S. Daniel, M. E. Callow, J. A. Callow and J. A. Finlay, *Biointerphases*, 2006, **1**, 18–21.

114 S. K. W. Dertinger, X. Y. Jiang, Z. Y. Li, V. N. Murthy and G. M. Whitesides, *Proc. Natl. Acad. Sci. U. S. A.*, 2002, **99**, 12542–12547.

115 W. Halfter, *J. Neurosci.*, 1996, **16**, 4389–4401.

116 D. Brunette, Principles of Cell Behavior on Titanium Surfaces and Their Application to Implanted Devices, in *Titanium in Medicine*, ed. D. Brunette, P. Tengvall, M. Textor and P. Thomsen, Springer, Berlin, Heidelberg, 2001, pp. 485–512.

117 T. P. Kunzler, T. Drobek, M. Schuler and N. D. Spencer, *Biomaterials*, 2007, **28**, 2175–2182.

118 T. P. Kunzler, C. Huwiler, T. Drobek, J. Vörös and N. D. Spencer, *Biomaterials*, 2007, **28**, 5000–5006.

119 C. B. Herbert, T. L. McLernon, C. L. Hypolite, D. N. Adams, L. Pikus, C. C. Huang, G. B. Fields, P. C. Letourneau, M. D. Distefano and W. S. Hu, *Chem. Biol.*, 1997, **4**, 731–737.

120 S. Daniel, S. Sircar, J. Gliem and M. K. Chaudhury, *Langmuir*, 2004, **20**, 4085–4092.

121 R. S. Subramanian, N. Moumen and J. B. McLaughlin, *Langmuir*, 2005, **21**, 11844–11849.

122 N. Moumen, R. S. Subramanian and J. B. McLaughlin, *Langmuir*, 2006, **22**, 2682–2690.

123 X. Yu, Z. Q. Wang, Y. G. Jiang and X. Zhang, *Langmuir*, 2006, **22**, 4483–4486.

124 A. D. Price and D. K. Schwartz, *Langmuir*, 2006, **22**, 9753–9759.

125 B. H. Clare, K. Efimenko, D. A. Fischer, J. Genzer and N. L. Abbott, *Chem. Mater.*, 2006, **18**, 2357–2363.

126 M. Y. M. Chiang, R. Song, A. J. Crosby, A. Karim, C. K. Chiang and E. J. Amis, *Thin Solid Films*, 2005, **476**, 379–385.

127 T. Künzler, PhD Thesis Nr 17049, ETH Zurich, 2007.